STRUCTURAL AND ELECTRONIC EFFECTS IN BaTiO$_3$

DUE TO THE Nb DOPING

Edgar Patiño and Arvids Stashans

Centro de Investigación en Física de la Materia Condensada, Corporación de Física

Fundamental y Aplicada, Apartado 17-12-637, Quito, Ecuador

Abstract. Some effects in BaTiO$_3$ due to the Nb-doping have been studied by means of the advanced quantum-chemical method based on the Hartree-Fock theory. A LUC (Larger Unit Cell) consisting of 135 atoms has been used. First, the effects in the cubic phase of the material have been investigated after the minimization of the total energy of the crystal. The obtained relaxation energy was found to be equal to 1.69 eV per LUC. An extra electron due to the Nb presence was found in the conduction band. In the tetragonal phase the relaxation energy is equal to 5.44 eV per LUC and an extra electron also jumps to the conduction band changing the state of the crystal.

1

INTRODUCTION

With no doubts $BaTiO_3$ is one of the most studied ferroelectric materials. Actually, the discovery of the ferroelectricity was done independently in various countries during the World War II [1] just in $BaTiO_3$ crystal. The reason of numerous investigations on $BaTiO_3$ is its remarkable properties in the tetragonal phase. It also has a high dielectric constant at ambient temperature [2]. This ceramic material shows piezoelectric properties as well. Another important features are its chemical and mechanical stability in a wide temperature range, which facilitates its fabrication in bulk polycrystals and both epitaxial and polycrystalline thin films [2]. All of these properties make this ceramic very useful in different applications such as dynamic random-access memories, piezoelectric transducers, thermistors and actuators [2]. In addition this titanate has large electro-optic coefficients and high photorefractive sensitivity, therefore can be used as an optical sensor [3].

Despite of the fact that many studies have been done so far on this ferroelectric material, there is still no complete understanding of the nature of many properties and phenomena in this material. For example, given the chemical formula of a perovskite material, there are no reliable methods for predicting transition temperatures. A number of questions without answer have produced very intensive theoretical studies of this ferroelectric material applying different techniques. Only few examples include first-principle ultrasoft-pseudopotential computations [4-6], the all-electron full potential linearized augmented-plane-wave studies of ferroelectricity in $BaTiO_3$ [7-10]. Recently studies of lattice dynamics using the variational density-functional perturbation theory [11] have been performed giving some important implications for the nature of the phase transitions and the dielectric and piezoelectric responses of this compound. Another

important studies involved [12-16] investigation of the role of electronic exchange-correlation energy in the stabilization of the different phases, examination of atomic charges, the phonon dispersion curves and variety of another problems. The majority of these studies are connected with the phase transition problems in $BaTiO_3$.

Following encouraging results obtained in our previous work [17], we study effects on different properties of $BaTiO_3$ due to the Nb-doping in both cubic and tetragonal phases. We apply the so-called single defect model within the periodic crystal model to investigate the influence of one point defect upon diverse properties in this ferroelectric material. For this aim we use quantum-chemical computations. Semi-empirical intermediate neglect of differential overlap (INDO) method modified for crystal calculations and the periodic LUC model as it is implemented into the CLUSTERD computer code are our tools [18]. Due to its semi-empirical character the computer program is not cumbersome and time consuming for treatment of electronic and spatial structures of complex systems, in particular, with a partially covalent chemical bonding, like oxide crystals [17]. Up to now the method has been successfully employed to investigate several perfect and defective oxides and materials with a simpler electronic band structure. It has important advantage of precise geometry prediction for impurity-doped crystals as it has been recently proved for a number of titanates like $BaTiO_3$ [17, 19], $SrTiO_3$ [20,21] and $CaTiO_3$ [22]. The computer code also was used in studies of another ferroelectric material, WO_3 [23].

The aim of this research is to study the influence of the Nb-doping upon the electronic band structure properties, as well as impurity effects on crystal geometry in both cubic and tetragonal phases.

DESCRIPTION OF THE METHOD

$BaTiO_3$ monocrystal has two phases, above 380 K it exists in cubic phase and it switches to tetragonal phase, or ferroelectric phase, below 380 K. In order to understand fully the effects of Nb doping, both phases need to be studied.

For this aim a quantum chemical method developed for crystal calculations has been used. This approach is based on molecular orbital (MO) theory [24], and the INDO approximation as it is implemented into the CLUSTERD computer code [18]. We have to underline that basically this method can be used for periodic systems, e.g., crystal computations. The method allows one to perform self-consistent-field (SCF) calculations of monocrystals containing different point defects, like in our case the $BaTiO_3$ crystal doped with the Nb impurity, which substitutes a Ti atom. Basically, our approach is a quantum-mechanical model, which solves the Schrödinger equation for a system of atoms fixed periodically.

In the Hamiltonian operator all Coulomb interactions between electrons and nuclei are considered, in addition to the exchange interaction. Adiabatic approximation is used in the method [25], i.e. the nuclei are considered motionless. Our investigation is done using a supercell of 135 atoms. This model is based on the so-called LUC approach, which has shown high reliability in point defect studies in a number of crystals. The use of a large size supercell (135 atoms) has the advantage of making impurity-impurity interaction negligible [17].

The main idea of the LUC method has to do with the so-called **k**=0 approximation. The information about the computational equations of the total energy of the LUC model is

given in [26]. Here we shall only outline the main ideas of the method. The Fock matrix elements are made self-consistent through density matrix elements obtained in the following manner:

$$P_{pq}^{0} = \frac{1}{N} \sum_{k} P_{pq}(\boldsymbol{k}) \exp(i\boldsymbol{k}\boldsymbol{R}_{v})$$

(1)

Here the summation is carried out over all **k** values in the reduced Brillouin zone (RBZ) of the LUC. In this way the information regarding the density matrix $P_{pq}(\mathbf{k})$ is obtained only in the point **k**=0. However, it has been argued [27] that, for sufficiently large cells, all the values of *k* points in the RBZ of the LUC will lie near *k*=0 so that it should be valid giving reliable results. Additionally, it has been demonstrated that several **k**-points in the RBZ are included in the calculation procedure on extending the primitive unit cell [26]. This means that density matrix elements $P_{pq}(\boldsymbol{k})$ are **k**-dependent and they are generated at each iteration, and then iterating to some predefined convergence criterion. Therefore, the calculation of the band structure in **k**=0 of the RBZ is equivalent to the calculation in several **k** points in the BZ of the primitive unit cell. It has been shown in many recent studies that an eightfold-symmetric extension of the primitive unit cell proves to be sufficient to reproduce almost exactly the electronic band structure of a given crystal [23,28,29]. In order to reduce the computational time certain semi-empirical parameters have been introduced. Owing to its semi-empirical nature and a specific parameterization scheme [30], CLUSTERD is not cumbersome and time consuming in the treatment of electronic and spatial structure of complex systems, specially the ones with mixed ionic-covalent chemical bonding like oxide crystals. The Fock matrix elements contain a number of semi-empirical parameters. The

5

diagonal matrix elements that consider the interaction of an electron of the ith valence atomic orbital (AO) of the atom A with its own core are taken in the following way:

$$U_{ii}{}^{A} = -E_{neg}{}^{A}(i) - \sum_{m}\left(P_{mm}{}^{(0)A}\gamma_{im} - \tfrac{1}{2}P_{mm}{}^{(0)A}K_{im}\right)$$ (2)

where P_{mm} are the diagonal elements of the density matrix, $E_{neg}(i)$ is the electronegativity of the ith AO, γ_{im} and K_{im} are one-center Coulomb and exchange integrals, respectively. The interaction between an electron of the ith AO of an A atom and the core of another atom B has the following form:

$$V_{iB} = Z_{B}\left[\frac{1}{R_{AB}} + \left(\langle ii|mm\rangle - \frac{1}{R_{AB}}\right)\exp(-\alpha_{iB}R_{AB})\right]$$ (3)

where α_{iB} is the parameter which considers the non-point character of the core B and diffuseness of the ith AO. R_{AB} represents the distance between atoms A and B while the $\langle ii|mm\rangle$ are two-center Coulomb integrals. The non-diagonal elements of Fock matrix contain the resonant integral parameter β_{AB}:

$$F_{im}{}^{\mu} = \beta_{AB}S_{im} - P_{im}{}^{\mu}\langle ii|mm\rangle$$ (4)

where ith AO belongs to atom A and mth AO belongs to atom B, μ means α or β spin subsystem, S_{im} is the overlap integral matrix and $P_{im}{}^{\mu}$ is the spin density matrix. The above described variables E_{neg}, $P^{(0)}$, α and β are adjustable semi-empirical parameters. Additionally, the parameterization scheme contains the fifth parameter ζ, which enters the exponent of the Slater-type AO. The parameterization is made by reproducing the following magnitudes: width of the forbidden energy gap, widths of the upper and lower valence bands, chemical composition of valence and conduction bands and lattice constants for both cubic and tetragonal structures. In particular, our obtained lattice constants a=4.01

Å for the cubic lattice and a=3.99 Å and c=4.03 Å for the tetragonal lattice, respectively, match exactly the experimental values [31]. However, the results of the electronic band structure and specially the bandwidths are somewhat different from the experimental observations. In particular, our ΔSCF calculated bandwidths were found to be equal to 5.8 eV and 5.6 eV for the cubic and tetragonal phases, respectively while the experimental magnitude stands for 3.2 eV [32]. Overestimation of the bandgap originates from neglecting the effect of the long-range electron correlation, which is a common fault of the methods based on the Hartree-Fock theory. It is believed that only short-range correlation corrections could be taken account through the semi-empirical atomic parameters. Long-range correlation between valence electrons is known to raise the upper valence band and lower the bottom of the conduction band leading to a reduction of the band-gap for oxide crystals by between 3 and 5 eV [33,34]. Thus obtained parameter sets for the $BaTiO_3$ crystal are given in Tables 1 and 2 and details of the parametrization of this crystal are described in one of our previous works [17].

The calculated energy bands composition for the $BaTiO_3$ crystal is in a very good accordance with the X-ray photoelectron spectra measurements [32]. In particular, as it follows from our computations, the chemical character of the lower valence band is mainly O 2s in nature while the upper valence band is predominantly O 2p in nature with a small admixture of Ti 3d AOs. The bottom of the conduction band is mainly composed of Ti 3d states with a small contribution of Ba 5s states.

The quantum-chemical method utilized in the present work has been successfully used in recent years for defect calculations in perovskite-type crystals including $BaTiO_3$

[17, 19], SrTiO$_3$ [20,21], CaTiO$_3$ [22] and KNbO$_3$ [35,36] and another complex oxide crystals like SiO$_2$ [26], α-Al$_2$O$_3$ [37,38], TiO$_2$ [39,40] and WO$_3$ [23].

RESULTS AND DISCUSSION

As it was mentioned above, the chemical character of the lower valence band of the cubic BaTiO$_3$ crystal obtained by the LUC computations is mainly O 2s while the upper valence band is predominantly O 2p in nature with small admixture of Ti 3d AOs. The bottom of the conduction band is composed of Ti 3d states mainly with a small contribution of Ba 5s states [17]. We observe some change in valence and conduction band compositions when study the tetragonal phase of the BaTiO$_3$ crystal. In particular, a larger amount of Ti 3d AOs is present in the upper valence and we find also a notable contribution of O 2p states in the lower part of the conduction band. This points out to the hybridization effect between Ti 3d and O 2p AOs, which accompanies the phase transition: cubic (paraelectric) $\rightarrow$ tetragonal (ferroelectric). These results are in very good agreement with another theoretical investigations of band structure properties in BaTiO$_3$ crystal. In particular, electronic structure calculations using the self-consistent-charge extended Hückel tight-binding method [41] and all-electron full potential linearized augmented-plane-wave computations [10] demonstrated importance of the hybridization between Ti 3d and O 2p orbitals for ferroelectricity in BaTiO$_3$ crystal.

In order to have an initial idea of how the atoms rearrange in the BaTiO$_3$ structure due to the Nb-impurity doping we use a LUC of 40 atoms (see Figure 1) for both cubic and tetragonal phases. The niobium replaces one of the titaniums located in the center of the LUC. The vicinity of defect (VOD) is thus composed of six oxygens and eight bariums as it

8

is shown in Figure 2. The performed calculations of the geometry optimization, e.g., the relaxation of the lattice, show similarity for both cubic and tetragonal phases. This is attained by the atomic displacements of the VOD since these atoms are closest to the impurity. The energy minimum is obtained by bariums' motion only. These atoms move outwards the niobium by a distance equal to 0.13 Å along the <111> directions preserving the symmetry of the system. That is their displacements are identical along x, y and z axes (see Figure 3). Because of these results it can be inferred that a LUC of 40 atoms is not enough to study Nb impurity and its influence upon different properties in the $BaTiO_3$ crystals. The oxygens in the VOD are the impurity-closest atoms and in principle they *should* experience at least a slight motion. Apparently we encounter so-called impurity-impurity mutual perturbation problem and its influence upon the reproduction of lattice distortion. Hence a bigger LUC should be used in order to neglect this artificial effect.

So, in the second step we utilize a LUC of 135 atoms with a structure similar to the one shown in the Figure 1. In this new set up the niobium is placed instead of one of the titaniums located in the middle of the supercell.

In the cubic phase the optimization of the geometry is attained by the impurity-outward displacements of bariums by a distance of 0.09 Å keeping the cubic symmetry of the VOD, e.g., we have <111> equal displacements along all three crystallographic axes. Employing the LUC of 135 atoms we find additionally that the oxygens entering the VOD experience displacements. Oxygens in the VOD have two of the three coordinates equal to the coordinates of the impurity atom. Therefore, their displacements are along <100> directions. The oxygens move towards the niobium impurity and this comes along with the hypothesis that we are dealing mainly with the electrostatic forces. This also shows that the predominant chemical bonding in $BaTiO_3$ has ionic character. Our anticipation is confirmed

during lattice relaxation since negative oxygens move towards the positive impurity by 0.02 Å. The amount of energy liberated by the system during relaxation, i.e., the relaxation energy, is found to be equal to 1.69 eV for the LUC composed of 27 primitive unit cells.

In the tetragonal phase the geometry relaxation is similar. The bariums move outwards the niobium by a distance of 0.09 Å. However, the direction of these movements are somewhat different from the one found for cubic phase. In particular, we observe displacements of bariums practically only in the x-y plane while the motion along the z axis is practically negligible. Oxygens in the VOD move towards the impurity by a distance of 0.01 Å but just along one axis (x or y) in analogous way to the previous case, i.e., their displacements along the z axis are too small. The relaxation energy obtained for this phase is equal to 5.44 eV, which is also for the extended LUC consisting of 27 primitive unit cells.

The summary of the geometry optimization for the two phases is given in Table 3. The directions of barium displacements are the same in both phases but the symmetry of their relaxation is appreciably different for the two phases. In tetragonal phase relaxation along the z axis is quite small while being greater along the x and y axes. Our explanation to the different relaxation energy of these atomic movements is connected with the lower compactness of the cubic phase relative to the tetragonal crystalline lattice. Perturbation by the same impurity can be felt stronger in more compact (tetragonal) lattice thus producing larger relaxation energy. Additionally, very large difference in relaxation energies for two phases partially can be explained by larger change in the chemical bonding in the tetragonal phase. As one can see from Table 4, change in atomic charges is larger for the atoms in the tetragonal structure, which leads to change in very strong ionic bonding for this phase. This could imply to larger relaxation energy in the tetragonal phase.

10

Another important outcome of our investigation is the atomic charge changes in the VOD region associated with the Nb-doping in the $BaTiO_3$ crystal. The atomic charges for both phases associated with the atoms closest to the impurity are given in Table 4. In the cubic phase, after doping, bariums practically suffer no change in its electronic density distribution. On the other hand the four oxygens, located along the z axis have an increase in its negative charge equal to 0.02 e compared to another oxygens entering the VOD. In our mind, this points out to the fact that niobium impurity can act as a center of new tetragonal phase since this effect occurs just along the z, i.e., the ferroelectric axis. The two titaniums closest to the impurity display the same charge change after doping. One can note the decrease of the positive charge for two defect-nearest titaniums. This effect is connected with the electron associated with the niobium impurity transfer from the local one-electron energy level within the band-gap to the conduction band. This effect will be discussed below.

In tetragonal phase the two impurity-closest titaniums and all bariums of the VOD have the same charges. Oxygens have different charges depending upon their location in the structure. We explain the differences in oxygen charges by lower point group symmetry of the tetragonal lattice and their location in different crystallographic sites.

Among the electronic properties of the doped crystal, the question to be answered is what happens with the extra electron imposed on the system by the niobium impurity? Due to the donor-impurity doping one could anticipate the occurrence of the local one-electron energy level within the band-gap. However, we observe rather surprising transfer of this extra electron to the conduction band of the material. This effect is observed in both phases. We have to note that the extra electron tends to remain in the conduction band, as it would be its natural or stable state. How is this natural state reached? During the relaxation the

11

system arrives to an intermediate state of the lowest energy (see Figure 4). In this state the electron still remains within the band-gap. Then during the SCF procedure the electron jumps to the conduction band, a new and final stable state of higher energy, in which the electron remains. It is important to note that the difference between energy levels for the cubic phase is equal to 0.3 eV. However, this difference increases up to 2.0 eV for the tetragonal phase. Where this energy came from? One possible answer for this question might come at glance suggesting that this energy came from electron-phonon interaction due to the relaxation of the system. However, our computer code does not consider directly this type of interaction. Therefore, in our mind this effect might be due to some structural properties of the material or it is related to some undiscovered phenomenon in this ferroelectric material. We are still working on this question.

Finally, we should note that experimentally it is known that due to the Nb-doping in the $BaTiO_3$ the conductivity shifts from a pure p-type semiconductor to an n-type semiconductor [42]. The increase in the electrical conductivity if niobium concentration is high enough is also well known effect in the $BaTiO_3$ crystal [43]. So, in our mind the electron transfer from the local level within the band-gap to the conduction band is directly related with the increase in electrical conductivity.

CONCLUSIONS

By means of the quantum-chemical method developed for periodic system, e.g., crystal computations we study Nb-impurity influence upon the structural and electronic properties of the $BaTiO_3$ crystal. The obtained very large relaxation energy in the tetragonal phase of the material is explained by more compact crystalline lattice of the tetragonal structure compared to the cubic one. The observed effect of the extra electron transfer from the local level within the band-gap to the conduction band might be attributed to the electrical conductivity augmentation in the Nb-doped material.

REFERENCES

1. A. von Hippel, <u>Rev. Modern Phys., 22</u>, 221 (1950).

2. D. Balzar, H. Ledbetter, P. W. Stephens, E. T. Park and J. L. Routbort, <u>Phys. Rev. B, 59</u>, 5 (1999).

3. U. van Stevendaal, K. Buse, S. Kämpar, H. Hesse and E. Krätzig, <u>Appl. Phys. B 63</u>, 315 (1996).

4. R. D. King-Smith and D. Vanderbilt, <u>Ferroelectrics, 136</u>, 85 (1992).

5. R. D. King-Smith and D. Vanderbilt, <u>Phys. Rev. B, 49</u>, 5828 (1994).

6. J. Padilia, W. Zhong and D. Vanderbilt, <u>Phys. Rev. B, 53</u>, 5969 (1996).

7. R. E. Cohen and H. Krakauer, <u>Phys. Rev. B, 42</u>, 6416 (1990).

8. R. E. Cohen and H. Krakauer, <u>Ferroelectrics, 136</u>, 65 (1992).

9. D. J. Singh and L. L. Boyer, <u>Ferroelectrics, 136</u>, 95 (1992).

10. R. E. Cohen, <u>Nature, 358</u>, 136 (1992).

11. P. Ghosez, E. Cockayne, U. V. Waghmare and K. M. Rabe, <u>Phys. Rev. B, 60</u>, 836 (1999).

12. P. Ghosez, X. Gonze and J. P. Michenaud, <u>Ferroelectrics, 206</u>, 205 (1998).

13. P. Ghosez, X. Gonze and J. P. Michenaud, <u>Ferroelectrics, 220</u>, 1 (1999).

14. P. Ghosez, J. P. Michenaud and X. Gonze, <u>Phys. Rev. B, 58</u>, 6224 (1998).

15. A. V. Postnikov, T. Neumann and G. Borstel, <u>Phys. Rev. B, 48</u>, 5910 (1993).

16. D. Khatib, R. Migoni, G. E. Kugel and L. Godefroy, <u>J. Phys.: Condens. Matter, 1</u>, 9811 (1989).

17. H. Pinto and A. Stashans, <u>Comput. Mater. Sci., 17</u>, 73 (2000).

18. E. V. Stefanovich, E. K. Shidlovskaya, A. L. Shluger and M. A. Zakharov, <u>Phys. Status Solidi B, 160</u>, 529 (1990).

19. H. Pinto, A. Stashans and P. Sánchez, <u>Defects and Surface-Induced Effects in Advanced Perovskites, NATO Science Series, High Technology</u> (Kluwer Academic Publishers, Dortrech, 2000), Vol. 77, p. 67.

20. A. Stashans and P. Sánchez, <u>Mater. Lett., 44</u>, 153 (2000).

21. A. Stashans, <u>Mater. Chem. Phys., 68</u>, 126 (2001).

22. F. Erazo and A. Stashans, <u>Phil. Mag. B, 80</u>, 1499 (2000).

23. A. Stashans and S. Lunell, <u>Int. J. Quant. Chem., 63</u>, 729 (1996).

24. J. A. Pople and D. L. Beveridge, <u>Approximate MO Theories</u> (McGraw-Hill, New York, 1970).

25. J. A. Pople, D. L. Beveridge and P. A. Dobosh, <u>J. Chem. Phys., 47</u>, 2026 (1967).

26. A. Shluger and V. Stefanovich, <u>Phys. Rev. B, 42</u> 9664 (1990).

27. A. H. Harker and F. P. Larkins, <u>J. Phys. C: Solid State Phys</u>., 12, 2487 (1979).

28. S. Lunell, A. Stashans, L. Ojamäe, H. Lindström and A. Hagfeldt, <u>J. Am. Chem. Soc., 119</u>, 7374 (1997).

29. A. Stashans, S. Lunell and R. W. Grimes, <u>J. Phys. Chem. Solids, 57</u>, 1293 (1996).

30. A. Shluger, <u>Theor. Chim. Acta, 66</u>, 355 (1985).

31. R. W. G. Wyckoff, <u>Crystal Structures</u> (Interscience, New York), 1960.

32. P. Pertosa and F. M. Michel-Calendini, <u>Phys. Rev. B, 17</u>, 2011 (1978).

33. A. B. Kunz, <u>Phys. Rev. B, 6</u>, 606 (1972).

34. P. W. M. Jacobs, E. A. Kotomin, A. Stashans, E. V. Stefanovich and I. Tale, <u>J. Phys.: Condens. Matter, 4</u>, 7531 (1992).

35. E. A. Kotomin, N. E. Christensen, R. I. Eglitis and G. Borstel, <u>Comput. Mater. Sci., 10</u>, 339 (1998).

36. E. A. Kotomin, R. I. Eglitis, A. V. Postnikov, G. Borstel and N. E. Christensen, <u>Phys.</u>

Rev. B, 60, 1 (1999).

37. A. Stashans, E. Kotomin and J.-L. Calais, Phys. Rev. B, 49, 14854 (1994).

38. P. W. M. Jacobs and E. A. Kotomin, Phys. Rev. Lett., 69, 1411 (1992).

39. A. Stashans, S. Lunell, R. Bergström, A. Hagfeldt and S.-E. Lindquist, Phys. Rev. B, 53, 159 (1996).

40. P. Persson, A. Stashans, R. Bergström and S. Lunell, Int. J. Quant. Chem., 70, 1055 (1998).

41. M. Kitamura and H. Chen, Ferroelectrics, 210, 13 (1998).

42. P. Moretti, G. Godefroy and J. M. Bilbault, Ferroelectrics, 37, 721 (1981).

43. M. Maglione and M. Belkaoumi, Phys. Rev. B, 45, 2029 (1992).

TABLE 1. Semi-empirical INDO parameter sets used in the present work: ζ (au), E_{neg} (eV), P^0 (*e*) and β (eV).

Atom	AO	ζ	E_{neg}	P^0	β
Ba	6s	1.65	6.2	0.2	-0.4
	5p	2.8	34.6	2.0	-4.0
Ti	4s	1.4	3.7	0.65	-0.5
	4p	1.1	-15.0	0.04	-0.5
	3d	1.93	7.2	0.55	-9.0
O	2s	2.27	4.5	1.974	-16.0
	2p	1.86	-12.6	1.96	-16.0
Nb	5s	1.55	24.5	0.8	-0.5
	5p	1.40	2.0	0.01	-0.5
	4d	1.35	23.7	0.017	-8.0

TABLE 2. Semi-empirical INDO two-center parameters α_{mB} (au^{-1}) optimized during the calculations, *m*th AO belongs to the atom A, where A≠B.

A	B			
	Ba	Ti	O	Nb
Ba	0.20	0.1	0.57	0.0
Ti	0.53	0.13	0.38	0.0
O	0.36	0.10	0.15	0.45
Nb	0.22	0.20	0.10	0.10

TABLE 3. Atomic movements (in Å) in niobium-doped $BaTiO_3$ crystal using the LUC consisting of 135 atoms. "+" and "-" denote outward and inward atomic displacements with respect to the impurity, respectively.

	Barium displacements	Oxygen displacements
Cubic phase	+0.09	-0.02
Tetragonal phase	+0.09	-0.01

TABLE 4. Atomic charges (in *e*) for the VOD atoms in the cubic and tetragonal phases, respectively. The numeration of oxygens corresponds to the one in Figure 2.

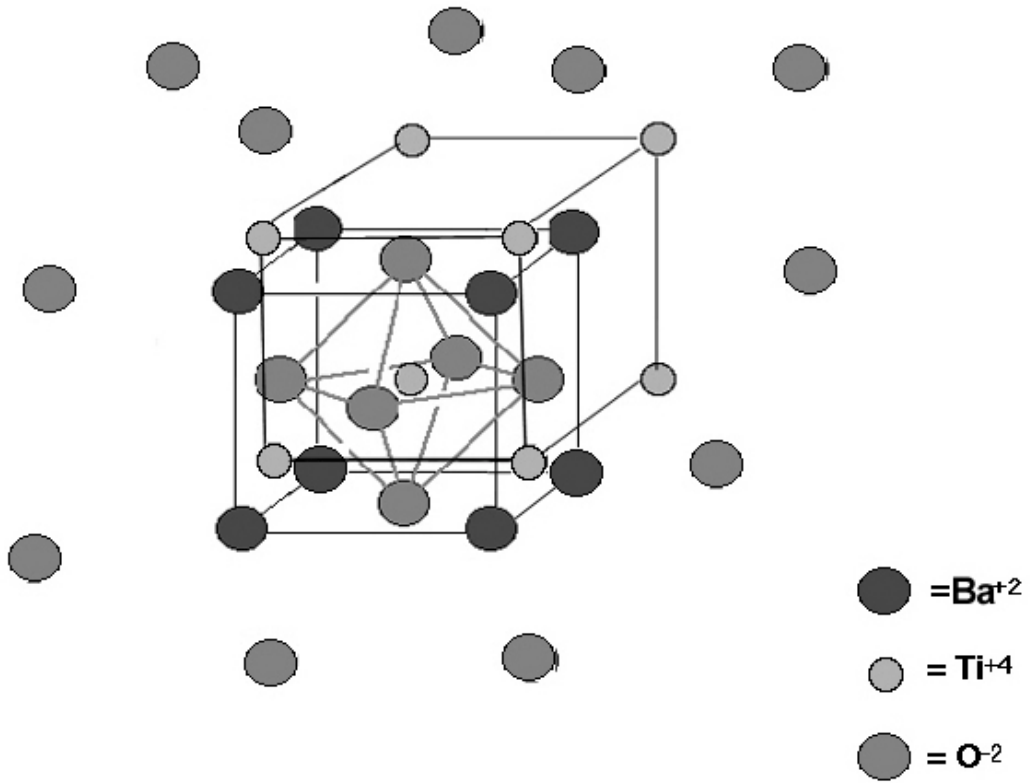|	Cubic phase		Tetragonal phase	
Atom	Pure crystal	Doped crystal	Pure crystal	Doped crystal
Bariums	1.88	1.88	1.88	1.89
Titaniums	2.13	1.92	1.90	1.68
O (1)	-1.33	-1.43	-1.26	-1.37
O(2)	-1.33	-1.41	-1.26	-1.42
O(3)	-1.33	-1.41	-1.26	-1.42
O(4)	-1.33	-1.41	-1.26	-1.39
O(5)	-1.33	-1.41	-1.26	-1.39
O(6)	-1.33	-1.43	-1.26	-1.39

FIGURE 1. 40-atomic LUC of the $BaTiO_3$ crystal used to obtain the first approximation of the lattice distortion pattern.
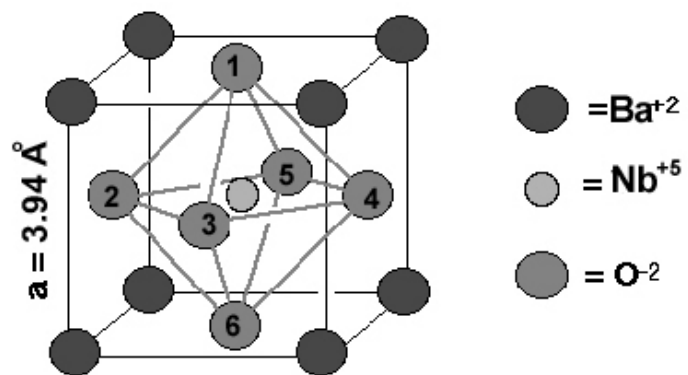
FIGURE 2. Vicinity of defect (VOD) composed of eight bariums and six oxygens. The niobium replaces one of the titaniums situated in the central part of the LUC.
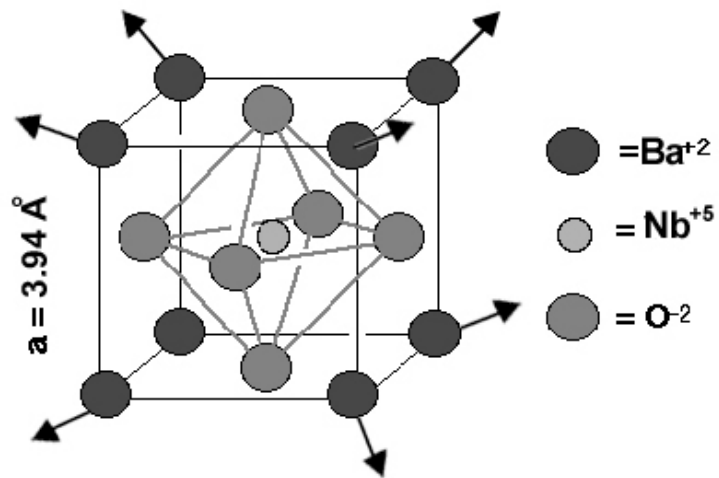
FIGURE 3. The relaxation of the structure due to the niobium impurity doping. The eight niobium-closest bariums move outwards while the six niobium-closest oxygens remain static pointing to the possible mutual Nb-Nb interaction.

FIGURE 4. The schematic drawing of electron transfer from the local one-electron energy level within the band-gap (intermediate state) to the conduction band (final state).
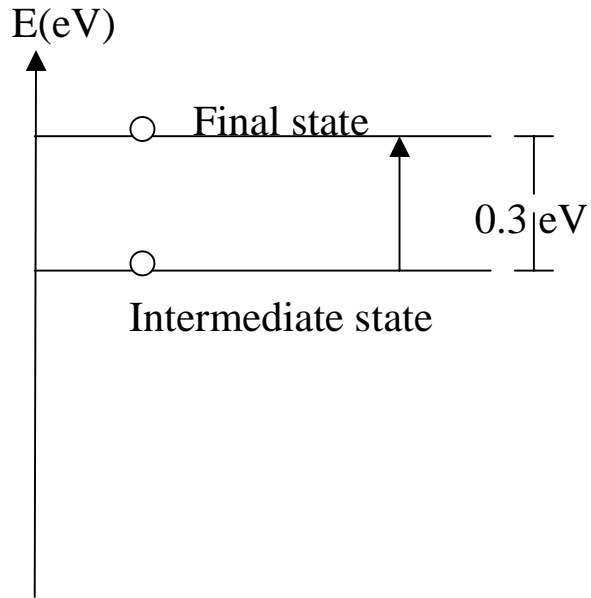
LUC of BaTiO$_3$

=Ba^{+2}

= Ti^{+4}

= O^{-2}

$a = 3.94$ Å

$= Ba^{+2}$

$= Nb^{+5}$

$= O^{-2}$

Cubic Phase   Tetragonal Phase

E(eV)

○   Final state   ○   Final State

                                              0.3 eV

○   2 eV
Intermediate state

                                    ○
                                    Intermediate state